

# Modelling and analysis of automotive A-pillar reinforcement using CFRP for high crashworthiness of passenger car

Vilas Kanthale<sup>1\*</sup>, and Jagmeet Singh Wade<sup>2</sup>

**Abstract.** In this work, an A-pillar component of an automotive car was studied for the safety of passengers and to avoid more damage to the vehicle. For this, a comprehensive model of an A-pillar with the reinforcement of carbon fiber was developed and analyzed using Finite Element Analysis (FEA) in ANSYS Workbench. Initially, the investigation was carried out on three materials such as structural steel without any reinforcement, epoxy glass fiber reinforcement, and carbon fiber reinforcement. Further, the 3-point bending test was performed without any orientation angle by using structural steel and carbon fiber material. Simulation tests were performed on a carbon fiber material with the orientation angles  $0^{\circ}$ - $0^{\circ}$ - $0^{\circ}$ ,  $0^{\circ}$ - $30^{\circ}$ - $60^{\circ}$ ,  $30^{\circ}$ - $60^{\circ}$ - $90^{\circ}$ , and  $90^{\circ}$ - $0^{\circ}$ - $90^{\circ}$  producing the reaction forces 16.046 KN, 16.988 KN, 16.945 KN, and 16.046 KN respectively. For validation, the experiments were conducted on carbon fiber components with a ply orientation angle of  $0^{\circ}$ - $30^{\circ}$ - $60^{\circ}$ , and the maximum reaction force generated 16.990 KN, which shows that this value is very close to the analytical analysis. Therefore, it is revealed that the strength and performance of the A-pillar component were enhanced with the use of carbon fiber as a reinforcement material compared with the structural steel.

## 1. Introduction

The A-pillar is a critical load-bearing component of the vehicle body, forming the forward boundary of the passenger compartment and providing structural continuity between the roof rail, windshield frame, and lower body structure. During frontal-offset collisions, side impacts, and rollover events, the A-pillar must sustain complex multi-directional loads to limit deformation and prevent intrusion into the occupant space. Its design is further constrained by the requirement to maintain adequate forward and lateral visibility for the driver. Any increase in cross-sectional thickness that improves crash performance simultaneously enlarges the blind zone, which is associated with elevated accident risk. Balancing structural integrity with visibility therefore makes the A-pillar particularly challenging to optimise compared with other pillars. Conventional steel A-pillars exhibit predictable ductility and energy absorption but contribute significantly to vehicle mass and often impose greater visual obstruction. Advances in lightweight materials have encouraged interest in carbon fibre reinforced polymers (CFRP), which provide high specific stiffness, favourable strength-to-weight ratios, and the capability to tailor mechanical behaviour by adjusting laminate architecture. These characteristics position CFRP as a promising alternative for A-pillar reinforcement in modern vehicles.

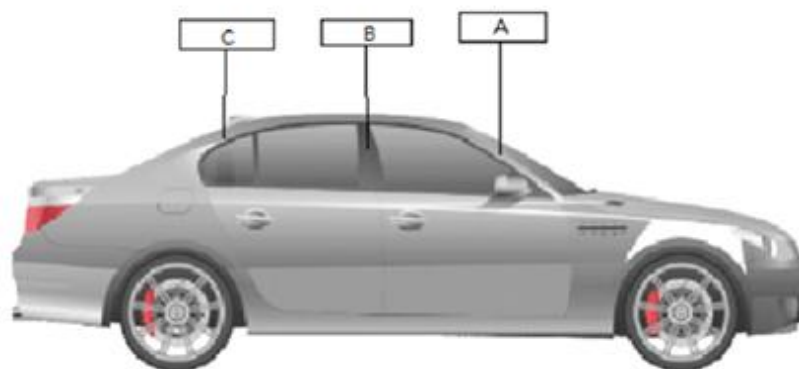


**Fig. 1.** Pillar Configuration A-B-C.

\* Corresponding author: [vilas.kanthale@mitwpu.edu.in](mailto:vilas.kanthale@mitwpu.edu.in)

Prior research on structural pillars has largely concentrated on the B-pillar, owing to its dominant role in side-impact protection. Studies investigating aluminium and magnesium alloys have demonstrated improved stiffness characteristics relative to steel [1], while composite B-pillar investigations validated through three-point bending have shown clear gains in strength-to-weight performance [2]. Work by Sun et al. further established that CFRP structural members can reduce component mass substantially without compromising stiffness [4]. Hybrid material systems combining high-strength steel with carbon-fibre composites or polymer-reinforced structures have also been examined, demonstrating improvements in crash energy management and weight reduction [11,16]. These findings collectively indicate a strong potential for composite materials in automotive structural applications.

In contrast, research focused specifically on the A-pillar is comparatively limited, despite its dual function in visibility and occupant protection. Mahoso et al. evaluated hybrid polyamide–steel A-pillar designs for enhanced rollover resistance [17], and Kyriazis et al. studied A-pillar geometries optimised for additive manufacturing using modal and static analyses [18]. Vaidya et al. further demonstrated that the application of CFRP to A-pillars can reduce obstruction angles significantly while lowering mass [30], reinforcing the relevance of composites for visibility-critical structures. Although these studies highlight the potential benefits of lightweight materials in A-pillar applications, they do not examine the influence of CFRP laminate orientation on A-pillar flexural behaviour. Given the anisotropic nature of CFRP, fibre orientation plays a decisive role in governing stiffness, load transfer, and failure mechanisms.

Existing literature does not provide a systematic evaluation of multiple CFRP layup sequences applied to a realistic A-pillar geometry, nor does it integrate finite element analysis with controlled experimental validation to assess orientation-dependent bending response. Many prior investigations rely either on simplified flat composite coupons or full-vehicle simulations, neither of which isolates the laminate-level behaviour of the A-pillar. The distinctive curvature, tapering, and structural transitions present in an actual A-pillar introduce complex stress paths that cannot be accurately inferred from generic laminate testing alone. This gap underscores the need for controlled component-level studies capable of isolating orientation-specific behaviour under well-defined loading conditions.

Three-point bending is extensively used in composite research as a standard procedure for characterising flexural stiffness and load–deflection behaviour. The method provides a repeatable configuration that avoids the confounding variables inherent to full-vehicle crash simulations, such as joint flexibility, dynamic rate effects, and interactions between multiple structural members. Aligning the finite element boundary conditions with the experimental setup enables robust comparison between numerical predictions and physical results, ensuring that observed trends are attributable to laminate orientation rather than modelling artifacts.

The present study addresses the identified research gap by analysing a CFRP-reinforced A-pillar using four distinct ply orientations— $0^\circ/0^\circ/0^\circ$ ,  $0^\circ/30^\circ/60^\circ$ ,  $30^\circ/60^\circ/90^\circ$ , and  $90^\circ/0^\circ/90^\circ$ —and validating the simulation results through three-point bending experiments. By examining how fibre orientation influences reaction force, deformation, and structural stiffness within an actual A-pillar geometry, this research provides an orientation-specific, experimentally supported assessment that is absent from previous literature. The close correspondence between numerical and experimental results reinforces the reliability of the modelling approach and offers insight into the design of lightweight, crash-resistant composite A-pillars.

## 2. Details of Specimen

The A-pillar is located at the front of a vehicle's passenger compartment and plays a vital role in the car's structure. Its primary functions include providing essential support to the roof, and significantly contributing to the overall structural integrity of the vehicle. Moreover, in the event of a collision, the A-pillar acts as a protective barrier, preventing objects from intruding into the driver or passenger compartment. This helps to reduce the chance of injury to the vehicle's occupants. To have a comprehensive understanding of the A-pillar's properties, a combination of analytical and experimental methods are used. The dimensions of the specimen are taken from the existing A-Pillar model of the vehicle by the using process of reverse engineering. The final dimensions are shown in Fig. 2.

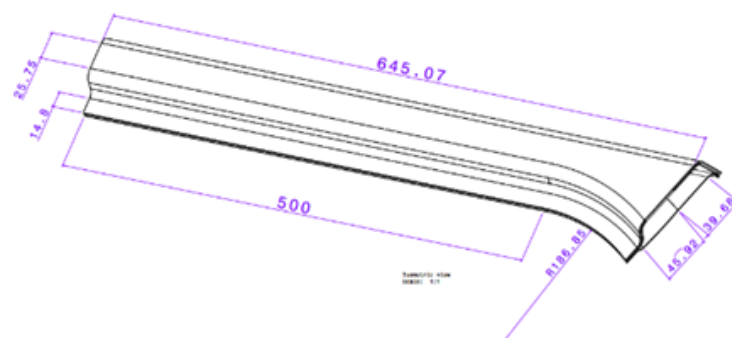


**Fig. 2.** Dimensions of Existing A-pillar.

After getting all dimensions, the next step is to develop a 3D CAD model, which is shown in Fig. 3.

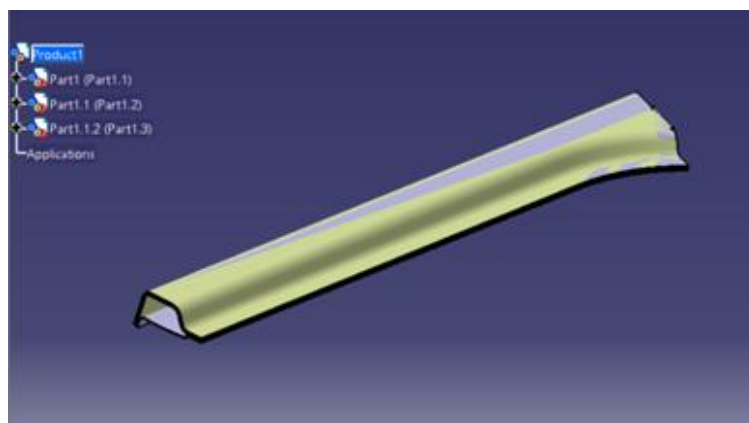


**Fig. 3.** CAD Model of Existing A-Pillar.

### 3. Modelling and Analysis by using FEA

#### 3.1 Finite Element Modelling

Finite Element Analysis (FEA) was performed using ANSYS Workbench to evaluate the structural response of the A-pillar under bending load. All models—steel and CFRP variants—were subjected to identical loading and boundary conditions for consistent comparison. The geometry was developed based on a three-point bending configuration, with both ends fixed and a 1 mm midspan displacement. Meshing was carried out using tetrahedral and hexahedral elements with an average size of 5 mm (Fig. 4).



**Fig. 4.** Meshing of A-Pillar in ANSYS.

This configuration offered a balance between computational efficiency and result accuracy. Mesh independence was verified by monitoring stress convergence. Each model had approximately 30,000–35,000 nodes and 14,000–16,000 elements.

#### 3.2. Boundary Conditions

The A-pillar was constrained at both ends to restrict translational and rotational motion, replicating fixed-support conditions. A vertical displacement of 1 mm was applied at the midpoint (Fig. 5). The same setup was retained across all test cases to ensure direct performance comparability.

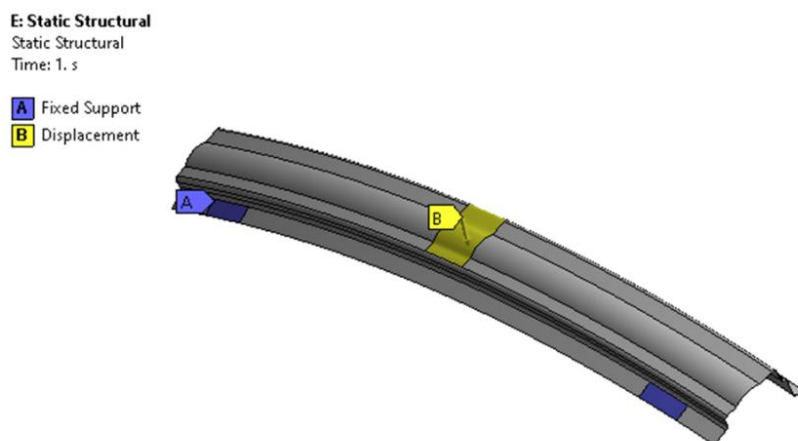


Fig. 5. Boundary Conditions for A-Pillar.

### 3.3. Analysis of Existing Structural Steel of A-Pillar

The baseline A-pillar, made of structural steel, exhibited a maximum deformation of **7.196 mm** under the applied displacement (Fig. 6).

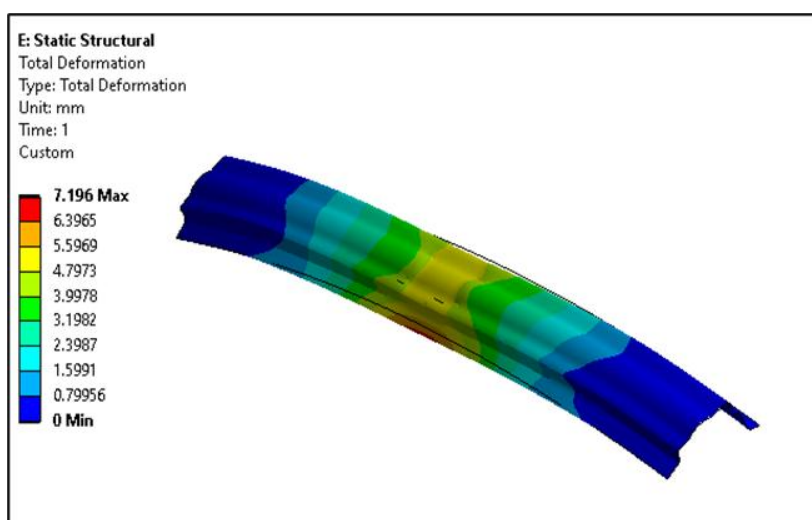
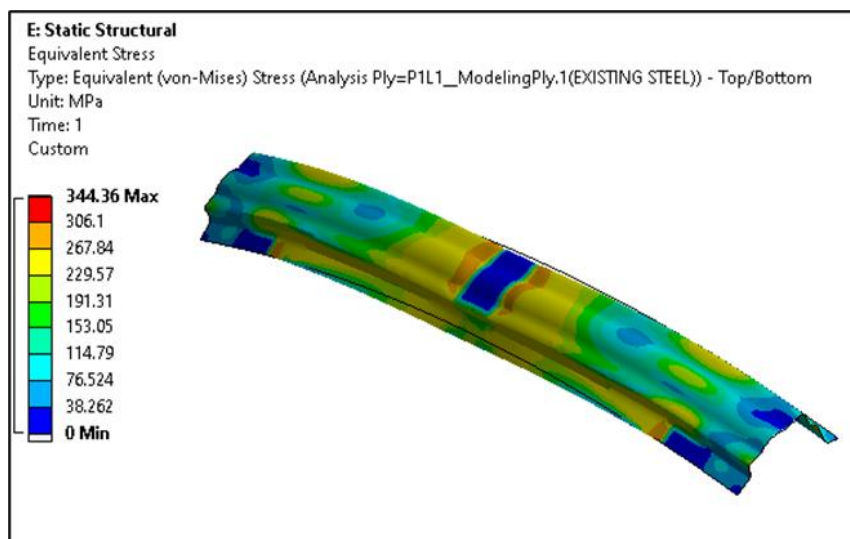


Fig. 6. Total Deformation Result of A-Pillar.

The maximum equivalent Von Mises stress reached **344.36 MPa** as shown in Fig. 7.



**Fig. 7.** Equivalent Stress Result of A-Pillar.

Equivalent stress results of A-pillar and the reaction force obtained was **7.8847 kN** as seen in Fig. 8.

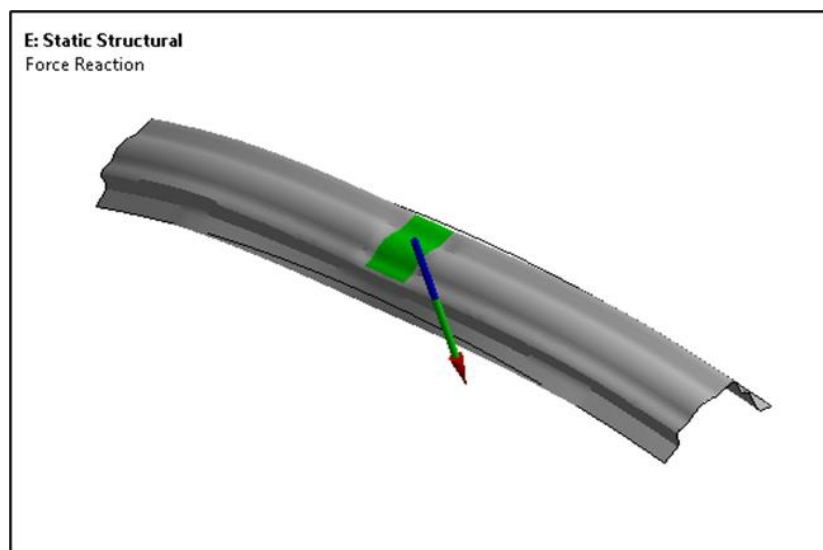


**Fig. 8.** Reaction Force Result of A-pillar.

The results show that steel, though ductile, experiences large deformation and moderate stress concentration, indicating limited stiffness and energy absorption potential under side loading.

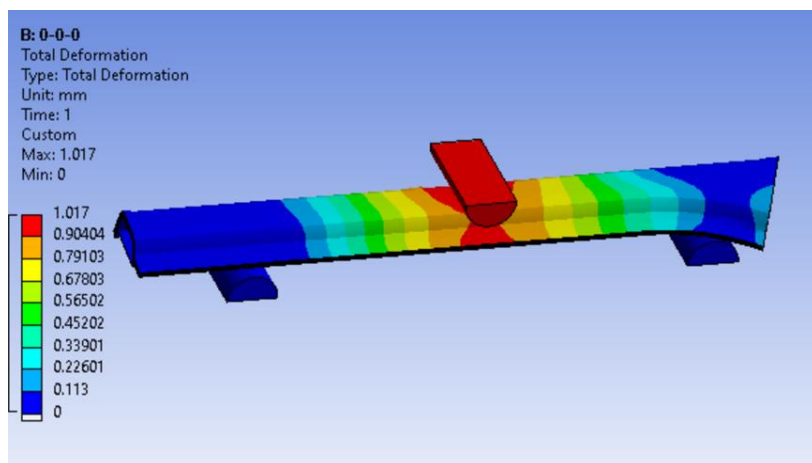
### 3.4. Effect of Different Ply Orientation Angles

The orientation angle is the degree to which an entity is twisted or positioned in relation to a traditional reference point, such as the north direction on a compass or the horizontal axis. The orientation angle is crucial in determining the preferred orientation of various attributes within the material's structure. When composite materials consist of different layers or fibers, the orientation angle is critical in determining the alignment direction of these fibers. This parameter has a substantial impact on the material's toughness, rigidity, and other mechanical properties.

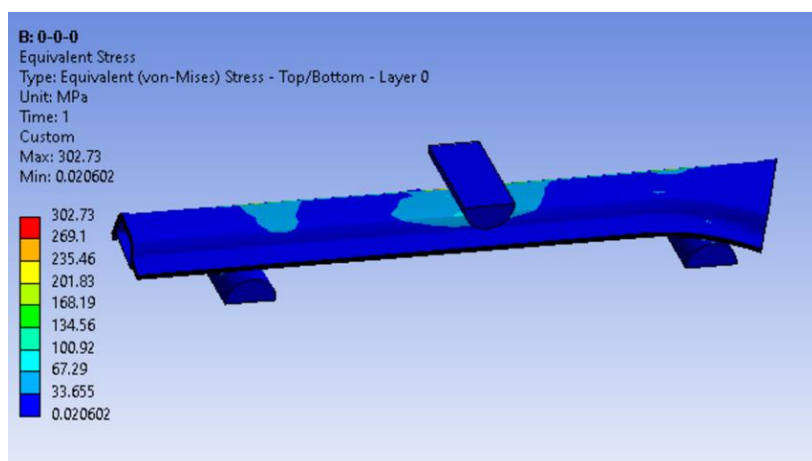
In order to observe the effect of different ply orientation angles, four specimens have with the different angles were analysed. The details are depicted as under.

### 3.4.1. Effect of Ply Orientation Angle of 0°/0°/0°

The A-pillar reinforced with carbon fiber composite (CFRP) showed a major improvement in structural performance. For the 0°/0°/0° orientation, total deformation decreased drastically to **1.017 mm** as shown in Fig. 9, while maximum stress reduced to **302.73 MPa** as shown in Fig. 10.

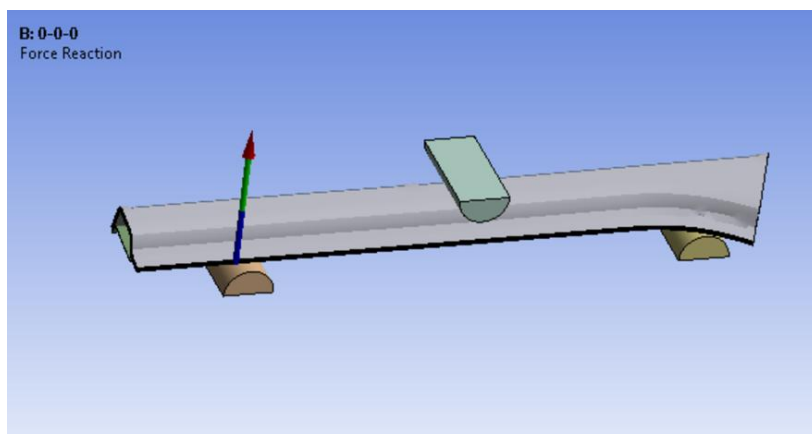


**Fig. 9.** Total Deformation of CF Reinforced A-pillar.



**Fig. 10.** Equivalent stress of CF reinforced A-pillar.

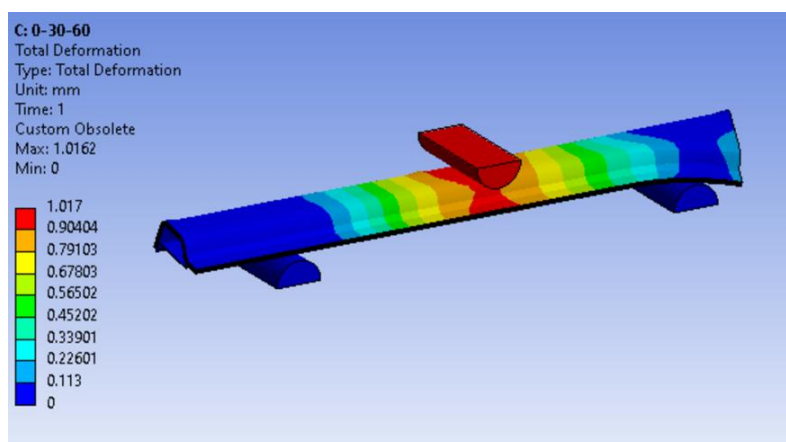
The corresponding reaction force increased to **16.046 kN** (Fig. 11), confirming enhanced stiffness and strength-to-weight performance.



**Fig. 11.** Force Reaction on A-Pillar.

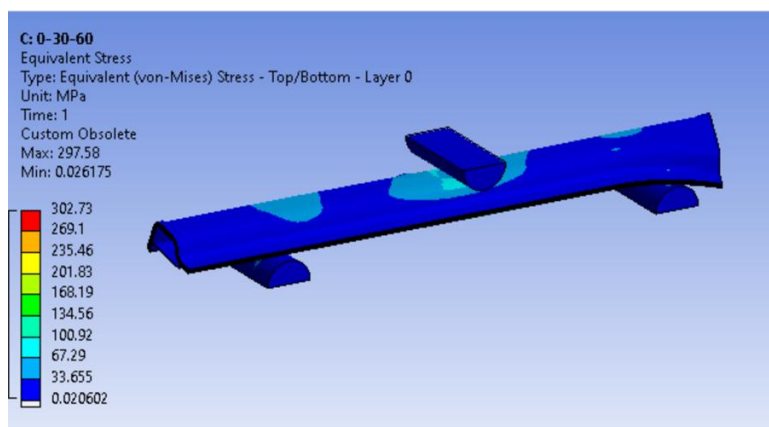
### 3.4.2. Effect of Ply Orientation Angle of 0°/30°/60°

Fig. 12 shows the geometry of the carbon fiber-reinforced A-pillar which has an orientation angle set to 0° 30° 60°. In this after applying 1 mm of displacement on the A-Pillar it gives 1.017 mm of total deformation.



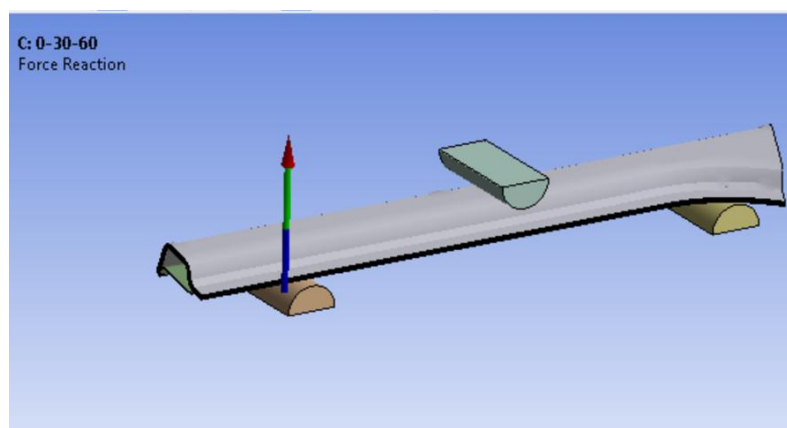
**Fig. 12.** Total deformation of carbon fiber reinforced A-pillar.

Further, an equivalent stress results with respective boundary conditions are shown in Fig. 13 and it gives the equivalent stress of 302.73 MPa after applying displacement.



**Fig. 13.** Equivalent Stress of Carbon Fiber Reinforced A-pillar.

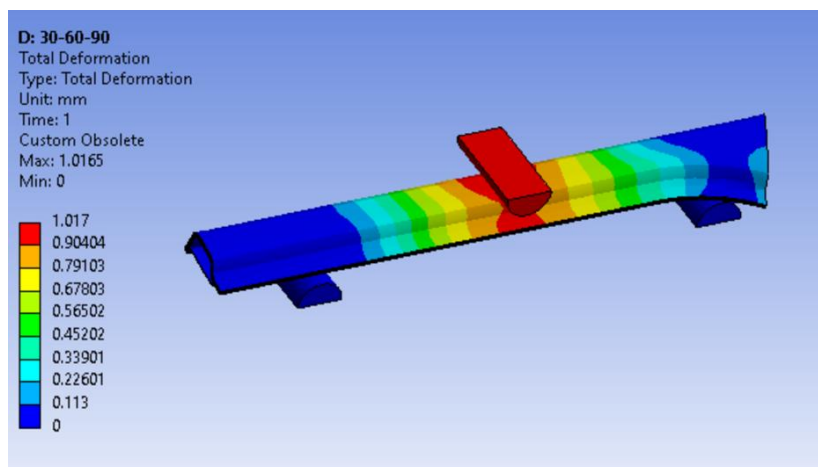
The Force reaction on carbon fiber reinforcement is shown in Fig. 14 and the maximum value over the period of time is 16988 N.



**Fig. 14.** Force reaction on carbon fiber reinforced A pillar.

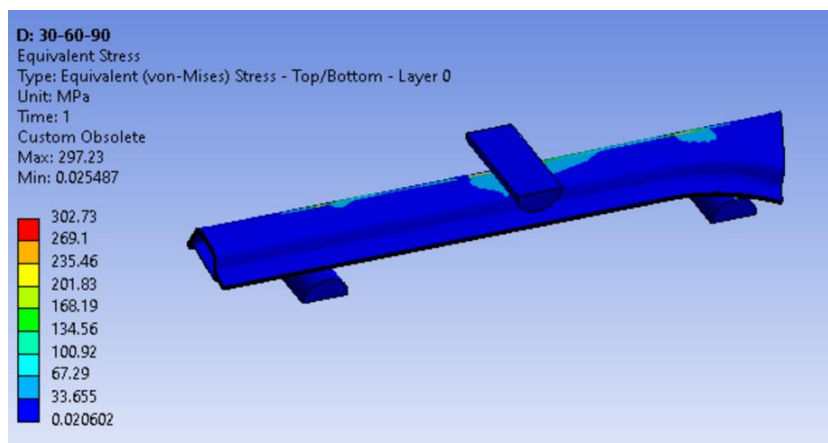
### 3.2.3. Effect of Ply Orientation Angle of 30°/60°/90°

In this after applying 1 mm of displacement on the A-Pillar, the total deformation occurred 1.017 mm as shown in Fig. 15.



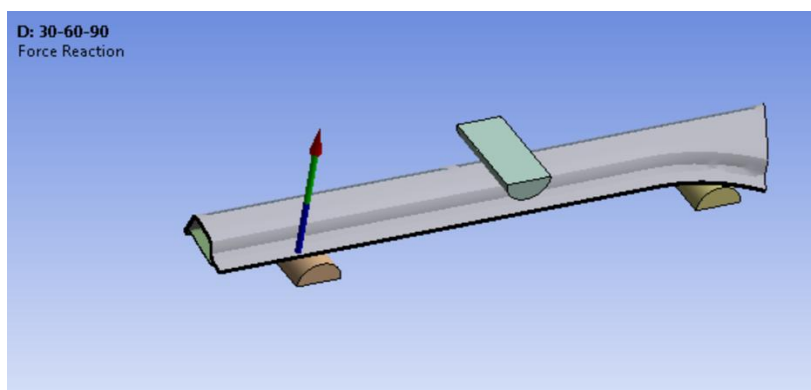
**Fig. 15.** Total Deformation of Carbon Fiber Reinforced A-Pillar.

Fig. 16 depicts the equivalent stress of a carbon fiber-reinforced of A-pillar, it gives the equivalent stress of 302.73 MPa after applying 1mm displacement.



**Fig. 16.** Equivalent Stress of Carbon Fiber Reinforced A-Pillar.

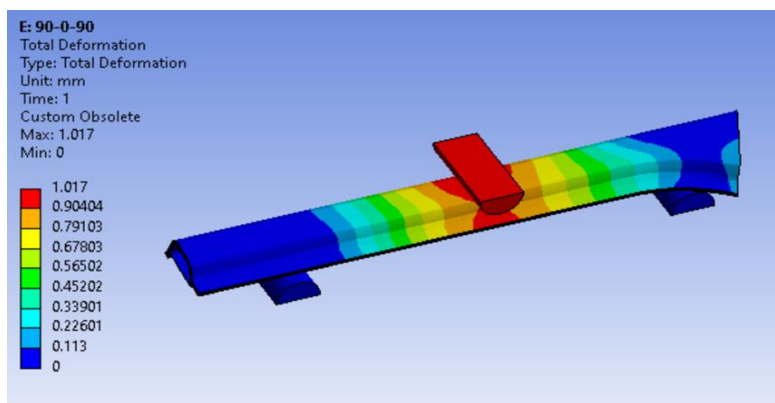
The force reaction that occurs on the A-pillar is shown in Fig. 17 For carbon fiber reinforce A – pillar maximum force reaction was 16.945 KN.



**Fig. 17.** Force Reaction on Carbon Fiber Reinforced.

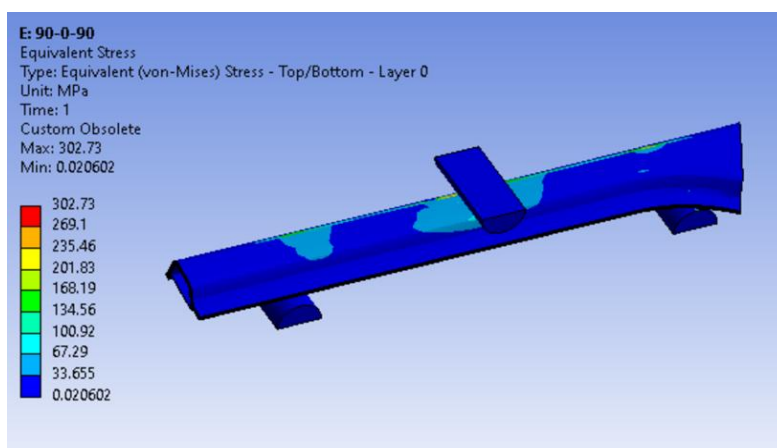
### 3.2.4. Effect of Ply Orientation Angle of 90°/0°/90°

In this, after applying 1 mm of displacement on the A-Pillar, the result shows 1.017 mm of total deformation as shown in Fig. 18.



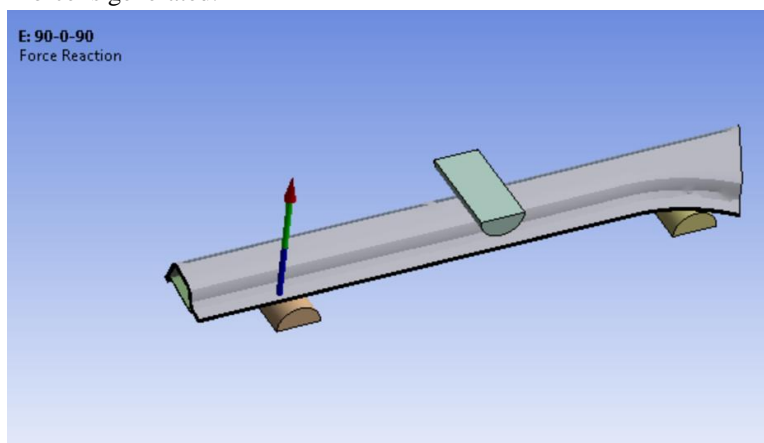
**Fig. 18.** Total Deformation of Carbon Fiber Reinforced A-Pillar.

Fig. 19 shows the equivalent stress of 302.73 MPa after applying displacement.



**Fig. 19.** Equivalent stress of carbon fiber reinforced A-pillar.

Fig. 20 depicts the force reaction that develops on the A-pillar as well as the highest level over time. Because of this, 16.046KN of reaction force is generated.



**Fig. 20.** Force reaction on carbon fiber reinforced.

### 3.5. FEA Results with Different Orientations

The orientation angle is extremely useful in engineering and materials science for determining the alignment of anisotropic materials or constructions. When tested in different directions, anisotropic materials exhibit diverging properties (e.g., mechanical, thermal, or electrical). In such cases when composite materials consist of different layers or fibers, the orientation angle is critical in determining the alignment direction of these fibers. This parameter has a substantial impact on the material's toughness, rigidity, and other mechanical properties. All models used identical mesh density and boundary conditions. Results are summarized in **Table 1**.

**Table 1.** FEA Results for Different Ply Orientations.

Orientation (°)	Max Reaction Force (kN)	Max Stress (MPa)	Total Deformation (mm)
Structural Steel	13.457	344.36	7.196
CFRP (0/0/0)	16.046	302.73	1.017
CFRP (0/30/60)	<b>16.988</b>	302.73	1.017
CFRP (30/60/90)	16.945	302.73	1.017
CFRP (90/0/90)	16.046	302.73	1.017

Among the tested configurations, the **0°/30°/60° layup** delivered the highest reaction force of **16.988 kN**, closely followed by the 30°/60°/90° stack. This orientation effectively distributes loads along multiple fiber axes, balancing axial, bending, and shear stiffness. The nearly identical deformation across all CFRP orientations reflects the laminate's uniform elastic behaviour, with fiber alignment mainly influencing load transfer efficiency.

The **force–response graph** (Fig. 21) illustrates the improvement in reaction force relative to the baseline steel pillar, clearly highlighting CFRP's superior load-carrying capacity.

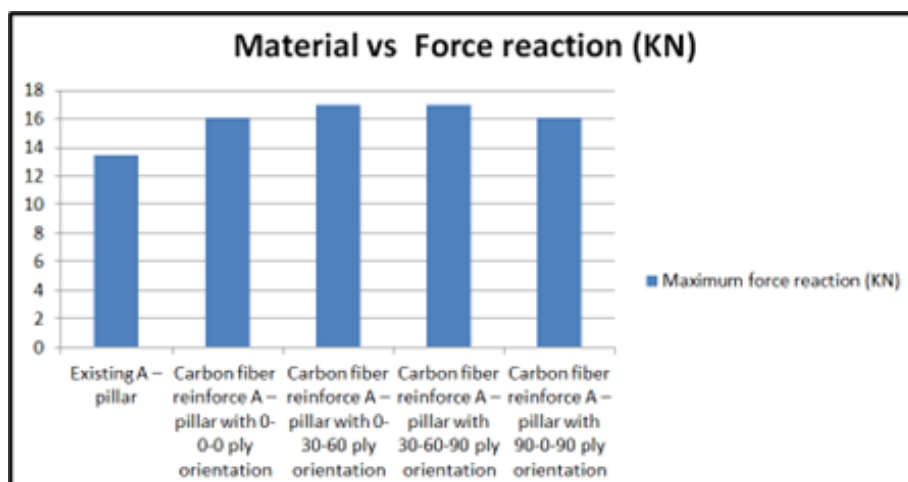


**Fig. 21.** Material V/s Force Reaction.

## 4. Experimental Analysis

The hand lay-up method is used in the creation of composite materials, such as fiberglass or carbon fiber-reinforced plastics (FRP/CFRP). This process includes layering reinforcing fibers, such as carbon fiber and fiberglass, within a mould and saturating them with a liquid resin to develop a composite specimen.

#### 4.1. Experimental Procedure

A universal testing machine (UTM) or universal tester is used to assess the mechanical properties of materials. It is vital in revealing material strength, stiffness, and other critical mechanical properties.

Fig. 22 shows the experimental set up. Specimen is put on a metal table of UTM after that load is applied for 1 mm of deformation. The loading system applies a regulated force to the specimen. As the specimen's behaviour is carefully studied, by applying force gradually on the specimen. This process culminates in the creation of a comprehensive and enlightening stress-strain curve, carefully plotting stress expressed as the meticulously applied force per unit area against the corresponding strain.

It is found during the experimentation that the specimens of the CFRP A-pillar ( $0^\circ/30^\circ/60^\circ$  layup) under a 1 mm displacement, the experimental reaction force recorded was **16.990 kN**, which is closely matches the simulated result of **16.988 kN**, confirming the fidelity of the FEA model as shown in Fig. 23.



Fig. 22. Experimental Set-Up.

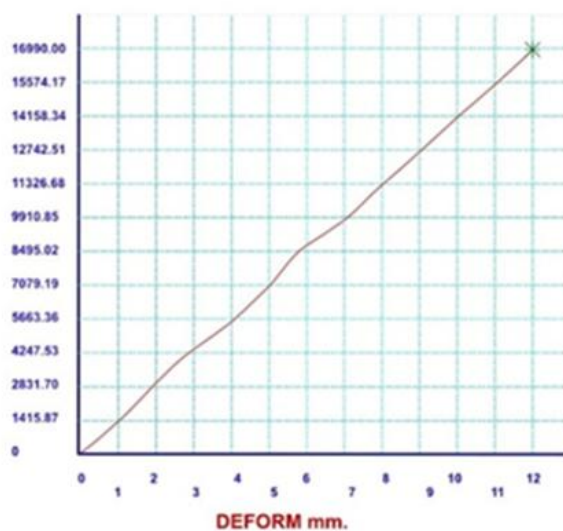


Fig. 23. Testing Graph.

The stress–strain curve demonstrated a linear elastic response up to failure, with no yield region, consistent with the brittle nature of CFRP. This agreement between simulation and experiment verifies that the modelling assumptions and material properties were accurately implemented.

#### 5. Conclusion

The comparative analysis demonstrates that CFRP significantly enhances A-pillar stiffness and load-bearing capacity while reducing deformation by nearly 85% compared to structural steel. The optimized  $0^\circ/30^\circ/60^\circ$  configuration balances longitudinal and transverse reinforcement, improving crash resistance without increasing thickness or weight. The experimental results revealed that the carbon fiber components with ply orientation angle  $0^\circ-30^\circ-60^\circ$ , the maximum

reaction force generated 16.990 KN, which shows that this value is very close to the analytical analysis. Therefore, it is revealed that the strength and performance of the A-pillar component were enhanced with the use of carbon fiber as a reinforcement material compared with the structural steel.

These findings suggest that substituting steel with carbon fiber composites can yield lighter, safer, and more visibility-friendly A-pillars for modern vehicles. Furthermore, consistent agreement between FEA and UTM results establishes confidence in the simulation methodology for future optimization studies.

## References

- [1] C. Venkataswamy, T. Naganna, N.K. Mishra, *Modelling and analysis of B-pillar*, *Int. J. Adv. Eng. Glob. Technol.* **3**, (2015).
- [2] M.I. Ibrahim, M.R.M. Rejab, H. Hazuan, M.F. Rani, *Finite element modeling and analysis of composite B-pillar*, *AIP Conf. Proc.* **2059**, 020022 (2019).
- [3] A.S. Gobir, A. Ikpe, E.K. Orhororo, *Design and reinforcement of a B-pillar for occupant safety in conventional vehicle applications*, *Int. J. Math. Eng. Manag. Sci.* **2**, 37–52 (2017).
- [4] D. Sun, C. Tao, *Lightweight study of carbon fiber composite B-pillar based on equal stiffness principle*, *Open Access Libr. J.* **5**, (2018).
- [5] K. Yu, Y. Liu, Z. Zhang, *Energy-absorbing analysis and reliability-based multi-objective optimization design of graded thickness B-pillar*, *Thin-Walled Struct.* **145**, (2019).
- [6] K. Hamza, K. Saitou, *Design optimization of a vehicle B-pillar subjected to roof crush using mixed reactive taboo search*, *ASME DETC Proc.* **2**, (2003).
- [7] A.E. Ikpe, I.B. Owunna, P. Satope, *Design optimization of a B-pillar for crashworthiness of vehicle side impact*, *J. Mech. Eng. Sci.* **11**, 2693–2710 (2017).
- [8] S.K. Basha, D. Kotte, S. Anudeep, C. Praveen, A.V. Subbarao, *Optimization of A and B pillars of automobile for crashworthiness*, *J. Adv. Res. Dyn. Control Syst.* **9**, (2017).
- [9] S. Joglekar, B.D. Patil, *Vibration analysis of composite reinforced B-pillar used in automobiles*, *Int. J. Innov. Res. Sci. Eng. Technol.* **6**, (2017).
- [10] N. Chase, R. Sidhu, *Optimization of a B-pillar undergoing roof crush using HEEDS COMPOSE*, *Red Cedar Technology*, AB 2036 (2012).
- [11] D.-J. Kim, J. Lim, B. Nam, H.-J. Kim, H.-S. Kim, *Design and manufacture of hybrid steel/carbon fiber composite B-pillar with high crashworthiness*, *Int. J. Precis. Eng. Manuf.-Green Technol.* **8**, (2021).
- [12] Y. Lin, J. Min, H. Teng, J. Lin, J. Hu, N. Xu, *Flexural performance of steel-FRP composites for automotive applications*, *Automot. Innov.* **3**, 280–295 (2020).
- [13] Y. Liu, Z. Zhu, Z. Wang, B. Zhu, Y. Wang, Y. Zhang, *Formability and lubrication of a B-pillar in hot stamping with 6061 and 7075 aluminum alloy sheets*, *Procedia Eng.* **207**, 723–728 (2017).
- [14] B. Hailu, T. Ashokkumar, *A new accident-proof material design for B-pillar of a car*, *Int. J. Chem. Tech Res.* **11**, 1–11 (2018).
- [15] J. Wei, L. Sun, W. Lv, J. Wang, Z. Wang, Y. Duan, L. Li, *Integrated design and experimental verification of assembly fiber reinforced thermoplastic plastics (AFRTP) automobile seat beams*, *Compos. Part B* **220**, 108968 (2021).
- [16] J.-H. Kang, J.-W. Lee, J.-H. Kim, T.-M. Ahn, D.-C. Ko, *Design of center pillar with composite reinforcements using hybrid molding method*, *Mater.* **14**, 2047 (2021).
- [17] R. Mahoso, S.S. Parihar, *Design and analysis of a polyamide-steel hybrid A-pillar for increased vehicle roof structural integrity in rollover accident scenarios*, *Int. J. Crashworthiness* **26**, (2019).

- [18] A. Kyriazis, D. Koulocheris, S. Polydoros, C. Vossou, *An AM-oriented vehicle chassis A-pillar design approach*, *MATEC Web Conf.* **318**, 01027 (2020).
- [19] G. Artner, W. Kotterman, G. Del Galdo, M.A. Hein, *Automotive antenna roof for cooperative connected driving*, *IEEE Access* **7**, 20083–20090 (2021).
- [20] S. Ben-Elechi, R. Bahloul, S. Chatti, *Investigation on the effect of friction and material behavior models on the springback simulation precision: application to automotive part B-pillar and material TRIP800 steel*, *J. Braz. Soc. Mech. Sci. Eng.* **44**, (2022).
- [21] J. Kurebwa, T. Mushiri, *A study of damage patterns on passenger cars involved in road traffic accidents*, *J. Robot.* **2019**, (2019).
- [22] S.K. Singh, *Road traffic accidents in India: Issues and challenges*, *Transp. Res. Procedia* **25**, 4708–4719 (2017).
- [23] S.W. Kirkpatrick, J.W. Simons, T.H. Antoun, *Development and validation of high-fidelity vehicle crash simulation models*, *Int. J. Crashworthiness* **15**, 395–406 (2010).
- [24] C. Wu, Y. Gao, J. Fang, E. Lund, Q. Li, *Discrete topology optimization of ply orientation for a carbon fiber reinforced plastic (CFRP) laminate vehicle door*, *Mater. Des.* **128**, (2017).
- [25] A.E. Ikpe, E.K. Orhorhoro, A.S. Gobir, *Design and reinforcement of a B-pillar for occupant safety in conventional vehicle applications*, *Int. J. Math. Eng. Manag. Sci.* **2**, 37–52 (2017).
- [26] R. Mahoso, S.S. Parihar, *Design and analysis of a polyamide–steel hybrid A-pillar for increased vehicle roof structural integrity in rollover accident scenarios*, *Int. J. Crashworthiness* **26**, (2019).
- [27] S. Toros, A. Polat, F. Ozturk, *Formability and springback characterization of TRIP800 advanced high strength steel*, *Mater. Des.* **41**, 298–305 (2012).
- [28] S. Repin, S. Evtiukov, S. Maksimov, *A method for quantitative assessment of vehicle reliability impact on road safety*, *Transp. Res. Procedia* **36**, 661–668 (2018).
- [29] X. Wei, H. Yuan, H. Wang, Y. Chen, *Intelligent design for automotive interior trim structures based on knowledge rule-based reasoning*, *Int. J. Automot. Technol.* **21**, (2020).
- [30] S. Vaidya, N.S.C. Velamakuri, P. Agarwal, S. Pilla, D. Schmueser, *Design and development of a composite A-pillar to reduce obstruction angle in passenger cars*, *SAE Int. J. Passeng. Cars-Mech. Syst.* **10**, (2017).